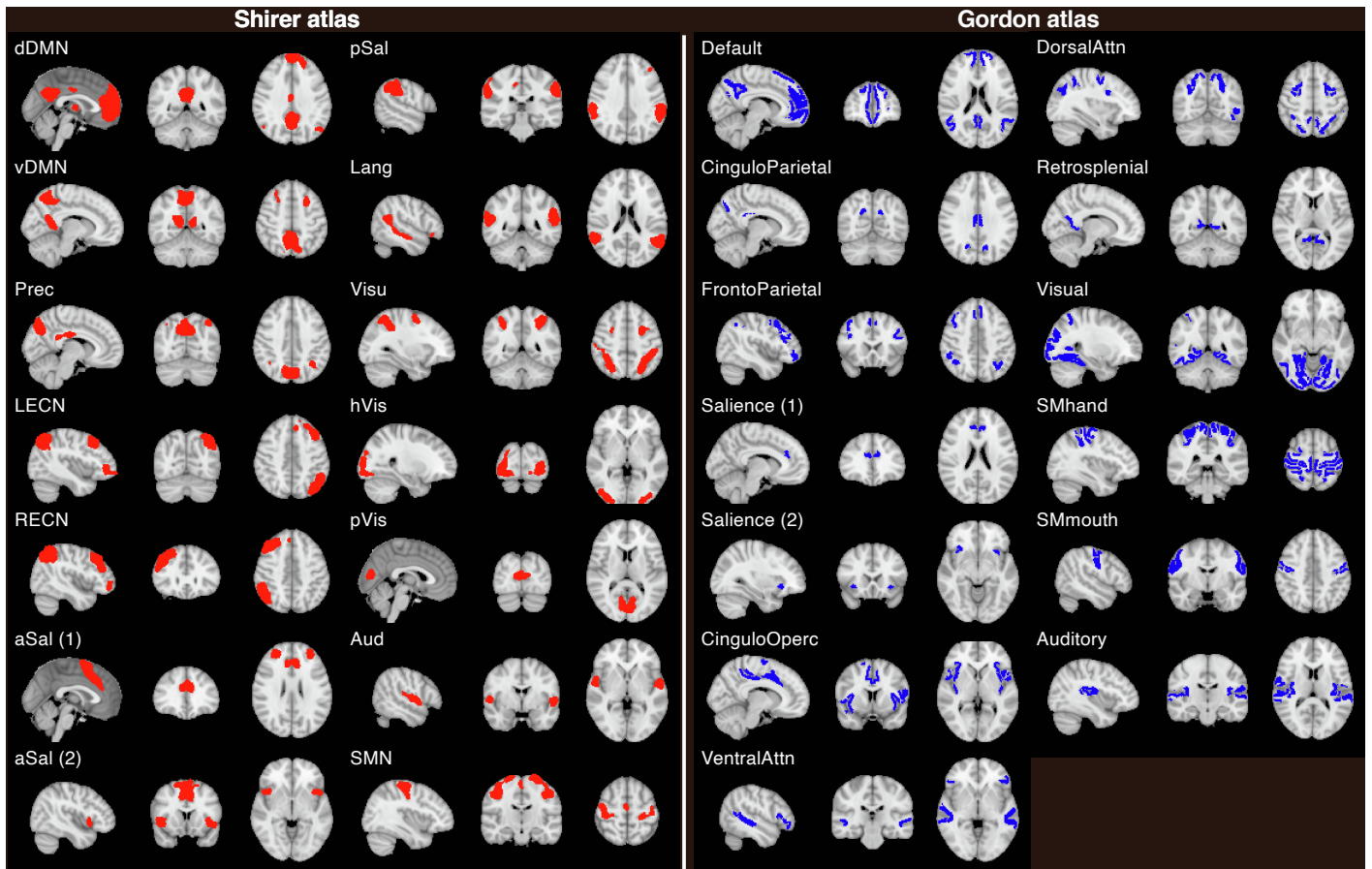


## **Supplemental information**

### **Bridging large-scale cortical networks: Integrative and function-specific hubs in the thalamus**

**Kazuya Kawabata, Epifanio Bagarinao, Hirohisa Watanabe, Satoshi Maesawa, Daisuke Mori, Kazuhiro Hara, Reiko Ohdake, Michihito Masuda, Aya Ogura, Toshiyasu Kato, Shuji Koyama, Masahisa Katsuno, Toshihiko Wakabayashi, Masafumi Kuzuya, Minoru Hoshiyama, Haruo Isoda, Shinji Naganawa, Norio Ozaki, and Gen Sobue**



**Figure S1. Atlases used in the analyses, Related to STAR Methods.**

Shirer atlas: dDMN, dorsal default mode network; vDMN, ventral default mode network; Prec, precuneus network; LECN, left executive control network; RECN, right executive control network; aSal, anterior salience network; pSal, posterior salience network; Lang, language network; Visu, visuospatial (dorsal attention) network; pVis, primary visual network; hVis, higher visual network; Aud, auditory network; SMN, sensorimotor network.

Gordon atlas: Default, default mode network; CinguloParietal, cingulo-parietal network; FrontoParietal, fronto-parietal network; Saliency, salience network; CinguloOperc, cingulo-opercular network; VentralAttn, ventral attention network; DorsalAttn, dorsal attention network; Retrosplenial, retrosplenial temporal network; Visual, visual network; SMhand, sensorimotor hand network; SMmouth, sensorimotor mouth network; Aud, auditory network.

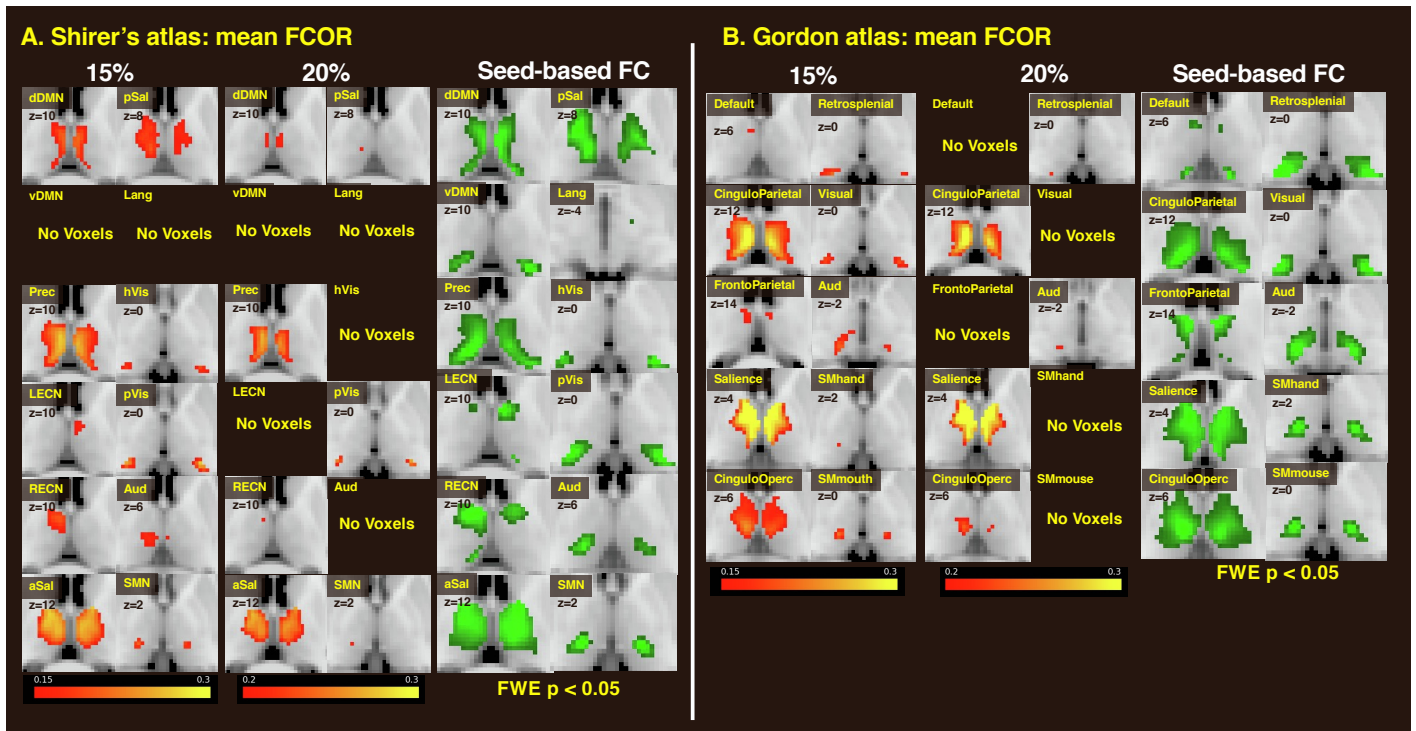


**Figure S2A. Regions above the threshold of mean FCOR in the thalamus (15% and 20%), Related to Figure 2.**

Regions shown in red-yellow indicate voxels with mean FCOR value across participants above 0.15 and 0.2 (15% and 20%) for resting state networks in (A) Shirer atlas and (B) Gordon atlas. Regions shown in green indicate voxels with significant functional connectivity from each resting state network, where significant voxels were thresholded at  $p < 0.05$ , corrected with family-wise error rate (FWE).

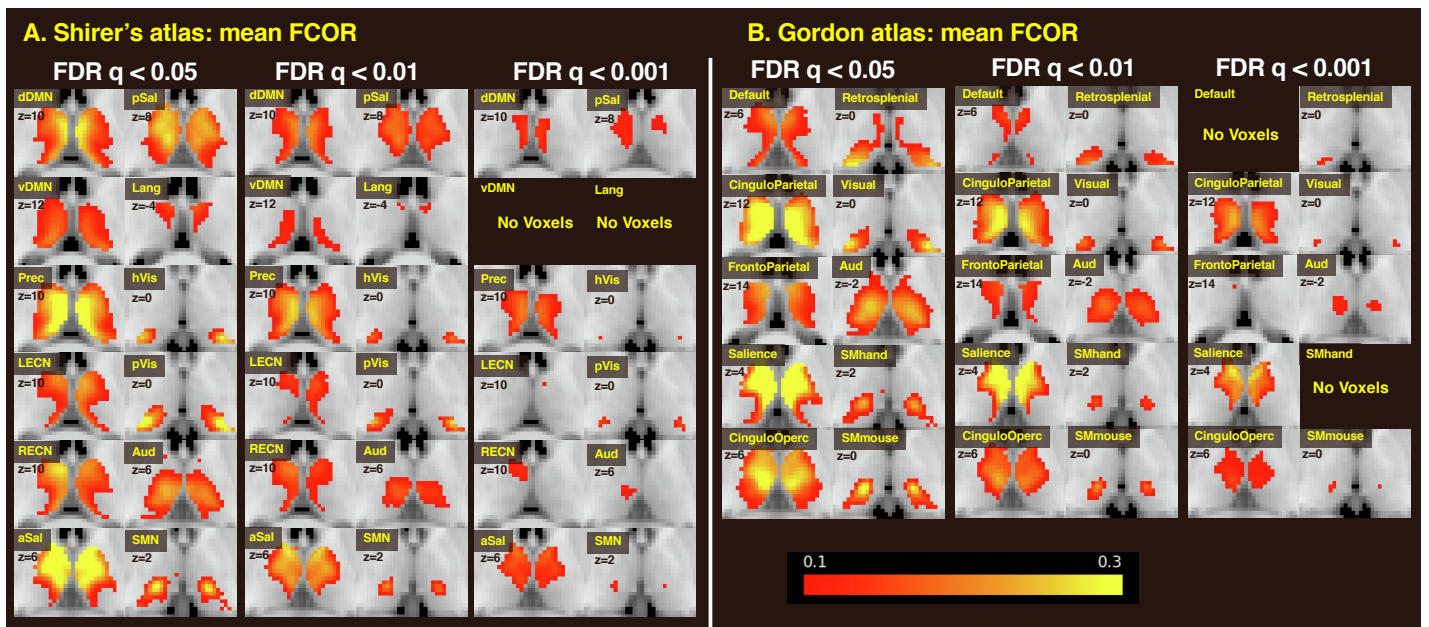


**Figure S2B. Regions above the threshold of mean FCOR in the thalamus (10%), Related to Figure 2 and STAR Methods.**

Individual FCOR maps were computed using different false discovery rate (FDR) threshold values (FDR  $q < 0.05, 0.01$  and  $0.001$ )

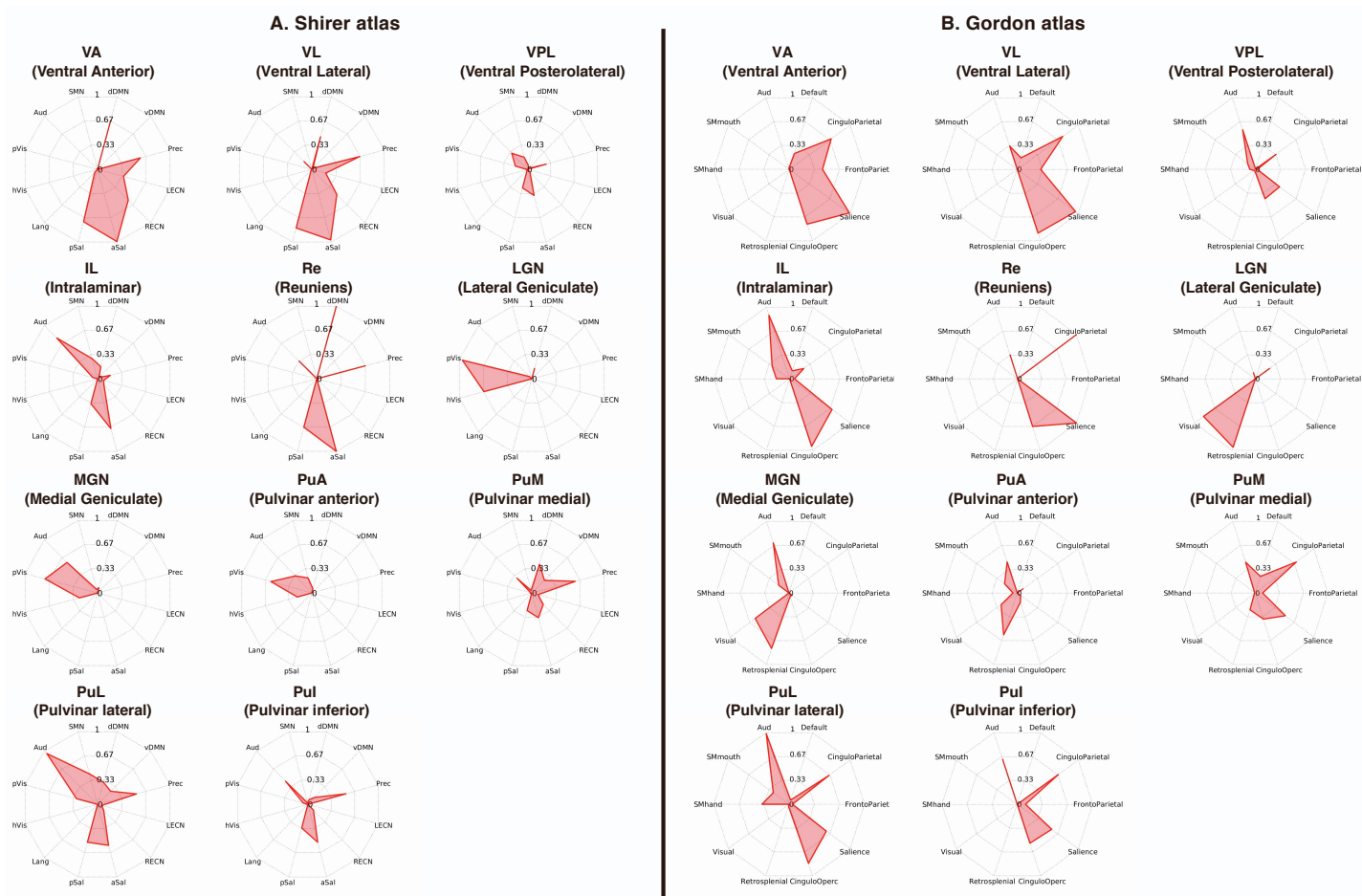


**Figure S3. Spider plots of FCOR values for different thalamic subregions, Related to Figure 5.**

Spider plots show the occupancy ratio of the different thalamic subregions for the (A) Shirer and (B) Gordon atlases.

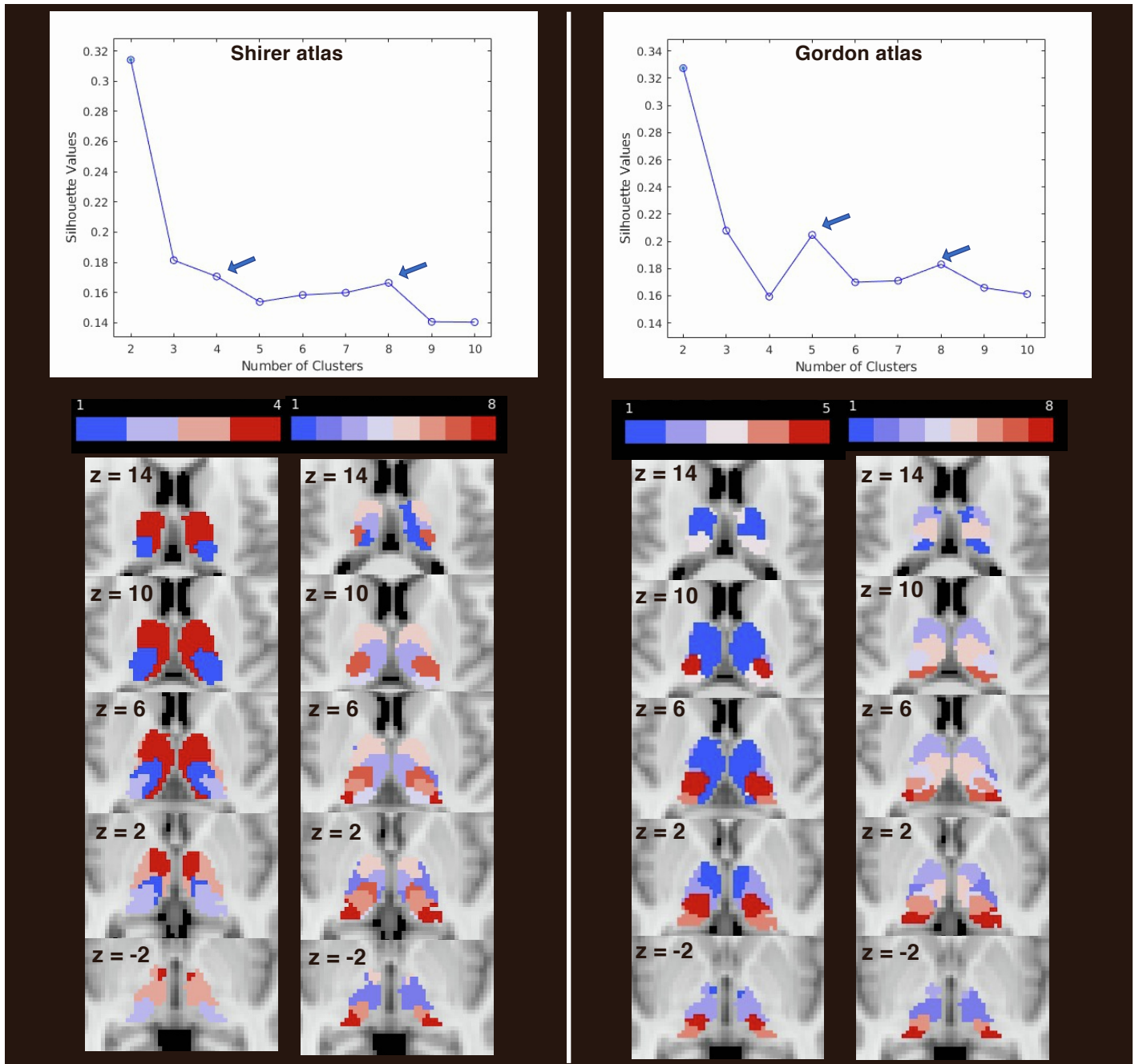


**Figure S4. k-means clustering of thalamic voxels using FCOR values as voxel features in the thalamus, Related to Figure 7.**

Upper line graphs show the mean silhouette value as a function of the number of clusters  $k$ . Arrows indicate the value of  $k$  with the third and fourth-highest silhouette values. Lower maps show the thalamic parcellations using  $k$ -means clustering with 4 and 8 clusters (Shirer atlas) as well as 5 and 8 clusters (Gordon atlas) using FCOR values generated using resting state network templates in the Shirer and Gordon atlases.

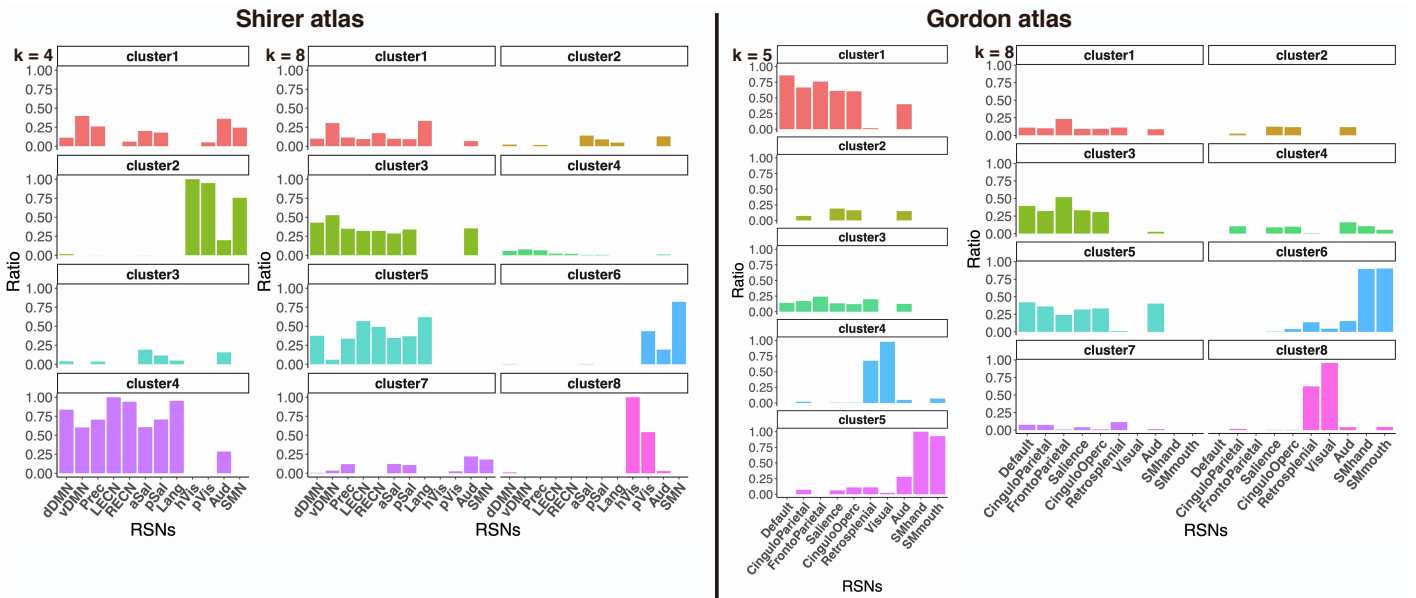


**Figure S5. The ratio of voxels within each parcel, shown in Figure S4, with strong (mean FCOR value > 0.1) connections to different resting state networks, Related to Figure 7.**

Bar graphs show the ratio of the 4- and 8-cluster parcellations in the Shirer atlas as well as the 5- and 8-cluster parcellations in the Gordon atlases.

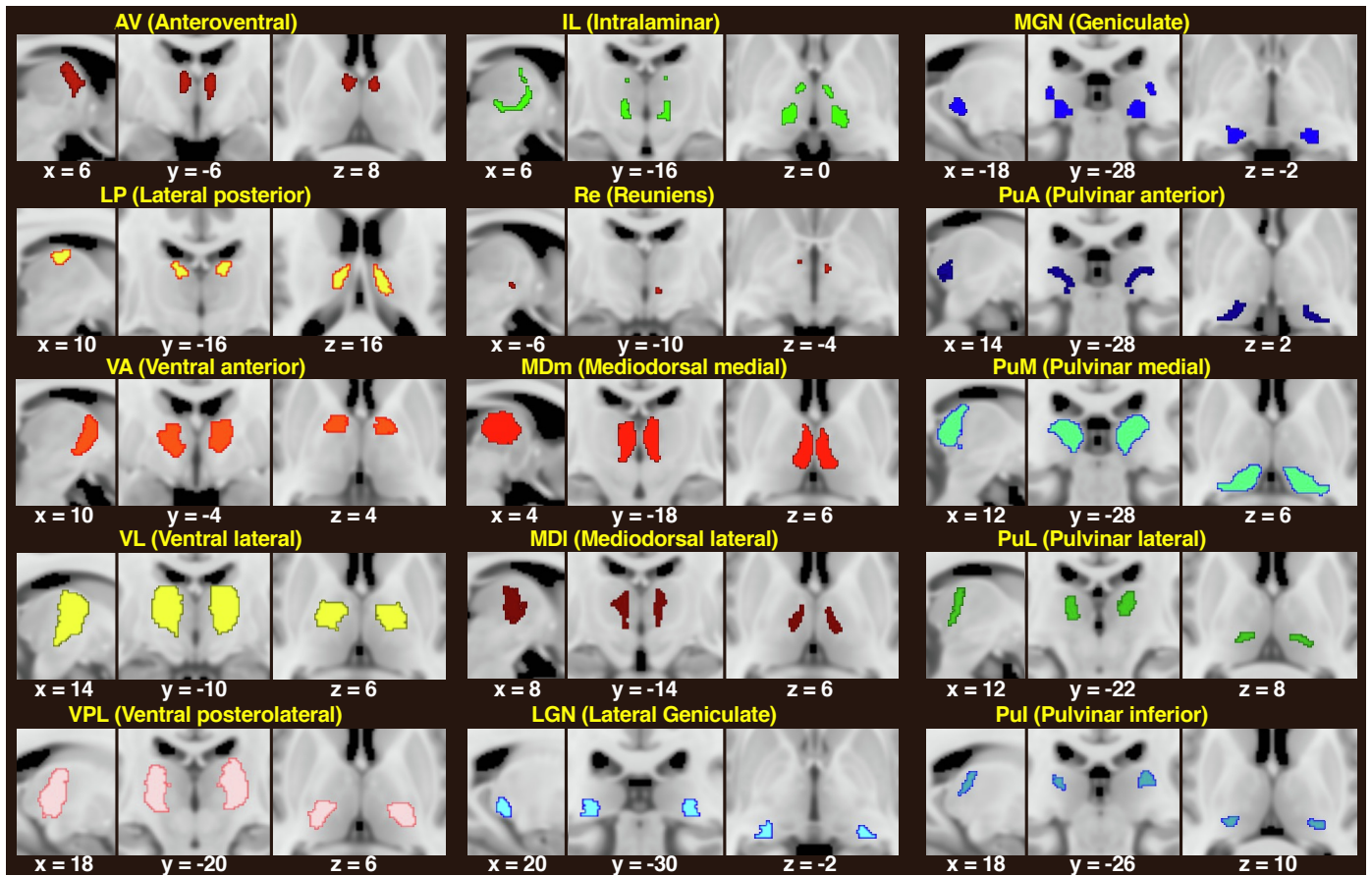


Figure S6. Thalamic subregions in the AAL3 atlas, Related to STAR Methods.